Progress In Electromagnetics Research M, Vol. 90, 19–26, 2020

A Novel Approach Using an Inductive Loading to Lower the Resonant Frequency of a Mushroom-Shaped High Impedance Surface

Minyu Gu, Daniel Vorobiev, Woo Seok Kim, Hung-Ta Chien, Hyun-Myung Woo, Sung Cheol Hong, and Sung Il Park*

Abstract—This paper reports a novel approach using an inductive loading to reduce the resonant frequency of a mushroom-shaped high impedance surface. The current path is extended on the mushroom-shaped structure's vias and additional traces, which introduces a three-dimensional inductor to the unit cell and leads to an increase in total inductance. As a result, the resonant frequency of the high impedance structure decreases, and a smaller unit cell size can be achieved at the low gigahertz frequency range. Finite element electromagnetic simulation, equivalent circuits modeling, and experimental measurements suggest the feasibility of the proposed approach.

1. INTRODUCTION

Society's insatiable demand for portable devices such as tablet pcs and smartphones has triggered research on compact antenna design targeting at fitting them in smaller packages. However, antenna designs based on established methods have reached their limits and face the competing requirements of maximizing radiated gain and minimizing near field coupling to the environment. For example, radiation incident on surface mounted antennas, such as patch antennas and bow-tie antennas, leads to surface currents on the outer metallic skin patch. To optimize radiation efficiency of the antenna, the substrate thickness needs to be quarter-wavelength. However, this is not feasible for compact antennas at all frequencies. Many studies have been done to overcome the issue. A mushroom-shaped high impedance surface is one of the solutions since it can offer the possibility of making the dimensions of surface-mounted antenna smaller [1–6]. A mushroom-shaped high impedance surface is a periodic structure that consists of a protuberant metal plate and a metal vertical via supporting the plate [1]. The period of the unit cell of the mushroom-shaped structure is designed to be much smaller than the wavelength of incident electromagnetic waves. Impedance on the surface of metal planes, which is defined as the ratio of the tangential component of the electric field to the tangential component of the magnetic field, is ideally zero. On the other hand, impedance on the surface of high impedance surfaces is ideally infinite. These high impedance surfaces have shown unique characteristics and potential usage in applications such as low-profile antennas and wireless power transfer [4, 7, 8]. One of the most interesting characteristics is that the high impedance surfaces suppress the surface waves and at the same time enhances the gain of antennas. This is referred as the reduction of the undesired side or back lobe and the reactive coupling to the nearby environment. If electromagnetic waves are incident on a metal surface, a 180-degree phase shift occurs on the surface. On the other hand, no phase shift or 0-degree phase shift occurs on a high impedance surface when electromagnetic waves are incident on the surface. This 0-degree phase shift makes for constructive interference between incident electromagnetic waves and reflected waves on the high impedance surfaces and contributes to the low profile of radiation patterns. In order to achieve these bandgaps, we must ensure that the total number of unit cells in the array is large enough to

Received 6 November 2019, Accepted 30 January 2020, Scheduled 10 February 2020
* Corresponding author: Sung Il Park (sipark@tamu.edu).
The authors are with the Department of Electrical & Computer Engineering, Texas A&M University, Texas 77840, USA.

emulate an array of infinite size. However, in reality, the total size of the high impedance surface is limited, and therefore the electromagnetic performance of the surface is degraded when the number of unit cell is accommodated for portable applications. Another issue involves feasibility of unit cell construction at a given dimension that meets quasi-static conditions [2]. Alternative mushroom-shaped structure with three stacked layers shows utility for use in wireless communication, however, a reduction in bandwidth prevents the widespread use of the structure in real applications [1].

Here, we propose a new mushroom-shaped structure with an inductive loading for lowering the resonant frequency of the high impedance surface. Vias and extended current paths lead to an increase in the inductance of a unit cell and thereby a shift in resonant frequency toward lower frequency ranges. Analytical modeling and numerical analysis provide guidelines for estimating a center resonant frequency. Experimental results via a vector network analyzer suggest that the proposed mushroom-shaped structure with an inductive loading can lower the resonance frequency and potentially reduce the unit size of the high impedance surface.

2. BACKGROUNDS

In the unit cell of the high impedance surface, the capacitive coupling between adjacent protuberant metal plates is linked to the fringe capacitance of the top metal plate while the inductive coupling is associated with the induced current around the 'open' loop, which consists of vias, metal plates, and the bottom ground. Figure 1(a) shows a unit cell of the traditional mushroom-shaped high impedance surfaces. The unit cell can be simply modeled to a parallel LC equivalent circuit as illustrated in Figure 1(d). The impedance of the circuit is given by Eq. (1) as follows [1].

$$Z = \frac{j\omega L}{1 - \omega^2 LC} \tag{1}$$

The impedance becomes very high and purely real at the resonant frequency. Both the transverse electric (TE) surface waves and the transverse magnetic (TM) surface waves are suppressed over the bandwidth centered at the resonant frequency. At frequencies below the lower band edge, the surface impedance is inductive and TM surface waves can propagate while at frequencies higher than that of the upper edge is capacitive and TE surface waves can travel.

Figures 1(b) and (c) show the proposed structure. For the traditional mushroom-shaped high impedance surface, a metal via vertically supports the top metal patch and makes an electrical connection between the metal patch and the ground plane. For the proposed structure, the via is divided into multiple sub-vias, each of which is connected by an extended current path. As shown in Figure 2, the extension of a current path from the edge of the metal path to the edge of the adjacent metal path contributes to a three-dimensional inductor as well as an increase in inductance. The current path is extended along the diagonal direction so that isotropic characteristics can be obtained. For the five-layered structure shown in Figure 1(c), the current path in the third layer is extended further so that maximum inductance can be achieved. The proposed high impedance structure here is designed to work at a low gigahertz range, with geometry parameters, $a = 5\,\text{mm}$, $g = 0.2\,\text{mm}$, $t = 3.175\,\text{mm}$.

The capacitance for a unit cell in the mushroom-shaped high impedance surface can be determined by Eq. (2), a formula for the fringe capacitance between two adjacent metal plates [9]. Here, ε_1 and ε_2 are the dielectric constants of air and substrate.

$$C = \frac{(a-g)(\varepsilon_1 + \varepsilon_2)}{\pi} \cosh^{-1}\left(\frac{2a-g}{g}\right) \tag{2}$$

The following describes the proposed approach for calculating an inductance of the three-dimensional inductor. In the two adjacent cells, an inductive current path consists of the top metal plates, sub-vias, extended current path, and surface as shown in Figure 2. The three-dimensional inductor highlighted by existing current paths can be decomposed into several square inductors, and the total inductance can be determined by Eqs. (3a) and (3b) [10]. Since the current direction is opposite for L_2 and L_3 shown in Figure 2(a), the mutual inductance is negligible and the total inductance becomes the summation of each individual one. The periodic nature of the high impedance surface allows for the use of an infinitely long solenoid model where the dimensions of a square solenoid are width (w) and height (h) and it has a unit current per length (L), and the inductance can be determined by

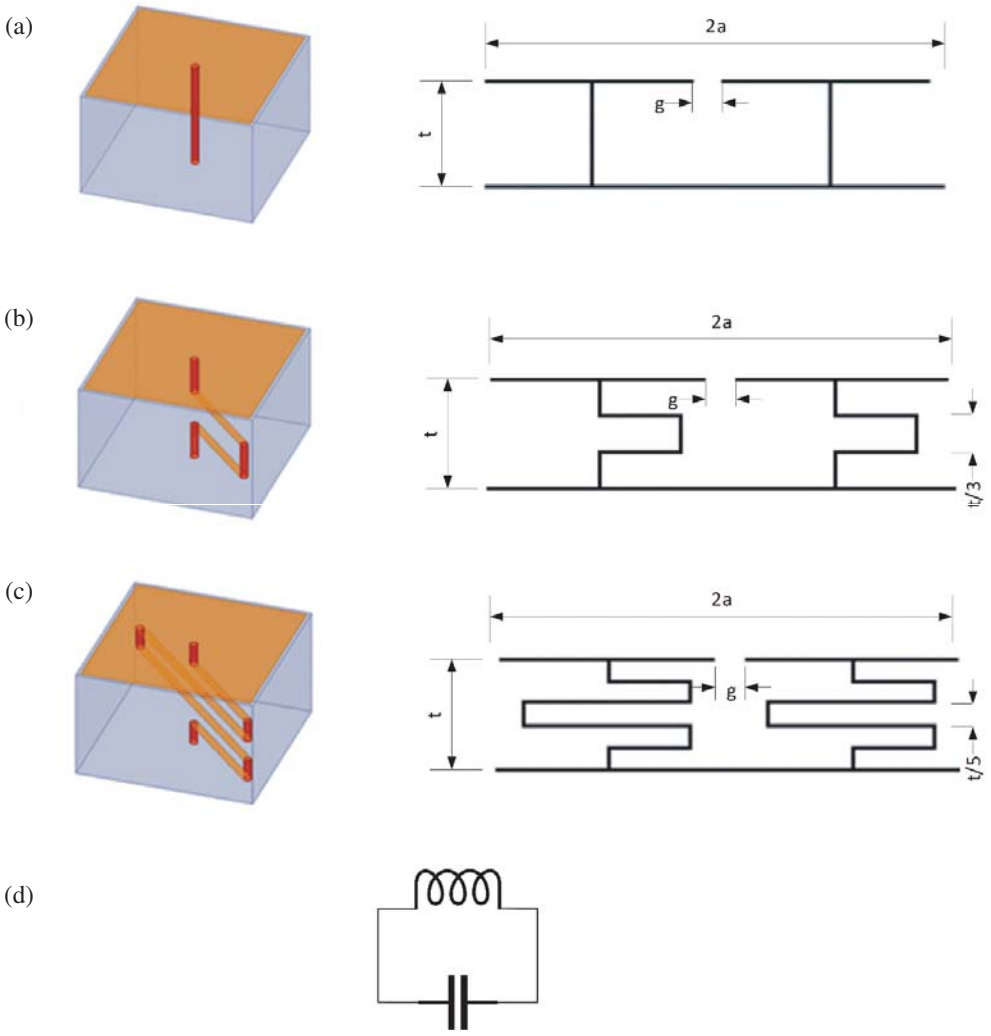

Figure 1. (a) Illustration of a unit cell and its cross-sectional view for a traditional mushroom-shaped high impedance surface, (b) the proposed three-layered surface with extended current paths, and (c) the five-layered surface with extended paths, respectively. (d) Equivalent LC circuit for a unit cell of the high impedance surface.

Eq. (3b). Based on the dimension given, the inductance for a traditional mushroom structure is simply $\mu_0 t$. Inductance for a three-layered structure shown in Figure 2(a) can be determined by Eq. (3c), and inductance for a five-layered structure shown in Figure 2(b) can be determined by Eq. (3d).

$$L = \sum_{i=1}^{m} L_i + \sum_{i=1}^{m}\sum_{j=1}^{m} M_{ij} \approx \sum_{i=1}^{m} L_i \tag{3a}$$

$$L_i = \mu_0 \frac{wh}{L} (i = 1 \ldots m) \tag{3b}$$

$$L_1 = \mu_0 t, \quad L_2 = L_3 = \mu_0 \frac{\frac{(a-g)}{2}\frac{t}{3}}{a} \tag{3c}$$

$$L_1 = \mu_0 t, \quad L_i = \mu_0 \frac{\frac{(a-g)}{2}\frac{t}{5}}{a} (i = 2 \ldots 7) \tag{3d}$$

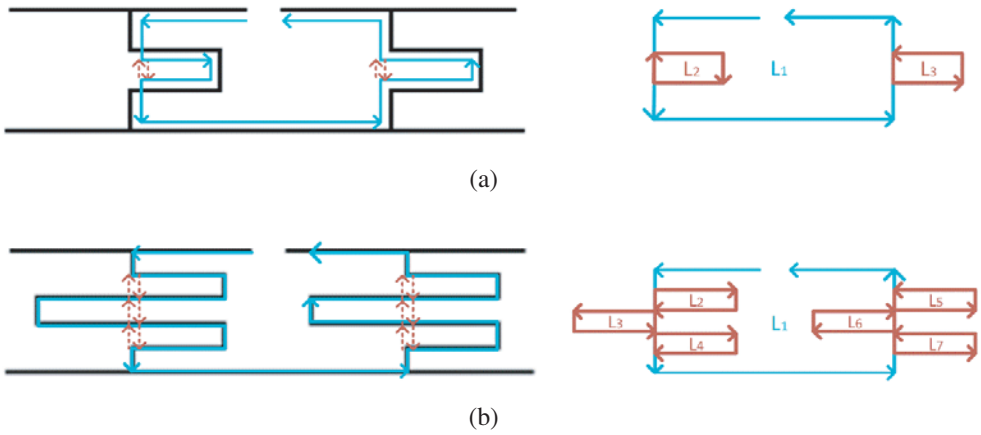

Figure 2. Illustration of decomposing the three-dimensional inductor into (a) three separate inductors, L_1, L_2, and L_3 for three-layered structure, and (b) seven separate inductors L_1 to L_7 for five-layered structure, respectively.

3. RESULTS

3.1. Equivalent Circuits Modeling

Resonant frequency calculations from the numerical and analytical approaches are summarized in Table 1. Results reveal that calculations from the analytical approach are in good agreement with numerical one. This suggests that extended current paths contribute to a large increase in the inductance, and thereby lower the resonant frequency of the high impedance surface. Note that the resonant frequency estimation of the five-layered structure led to a discrepancy of 17.4% between numerical and analytical approaches. Furthermore, its bandwidth is relatively narrow compared with the other two cases. This suggests that parasitic capacitive couplings between adjacent extended paths, ground planes, and top plates are no longer negligible as more layers are added at a given thickness of substrate. The result allows for further reduction in a resonant frequency of the multilayer mushroom structure. Here, our model relies on a simple LC structure and does not consider a parasitic capacitance. Therefore, similar level of discrepancy is not achieved in five-layer structures. One way to resolve this issue is to increase gaps between layers such that couplings between each layers are negligible. Please note that this parasitic capacitance could be beneficial for lowering the resonance frequency of high impedance surface at the cost of bandwidth reduction.

Table 1. The summary of the central resonance frequency from the numerical calculation, analytical approach, VNA S_{21} measurement data and inductance estimated from the analytical approach.

	Method	Normal-Structure	Three-Layered Structure	Five-Layered Structure
Central Resonant frequency (GHz)	EM Eigen Mode Simulation	4.755	3.976	3.011
	Circuits Modeling	4.438	3.863	3.535
	S_{21} Measurement	4.235	3.685	/
Inductance	Modeling Estimation (nH)	3.990	5.267	6.288

3.2. Simulation Results

We perform a computer simulation using a commercial finite element analysis tool, HFSS, to verify the proposed design prior to fabrications, and use Eigen analysis for a unit cell under linked boundary conditions from the sidewalls of a unit cell [11]. A via connecting the top metal plate to the bottom surface is embedded in an FR4 dielectric substrate and the top protuberant metal plate is not connected to adjacent plates. Perfect matched layer is inserted 15 cm away from the high impedance surface.

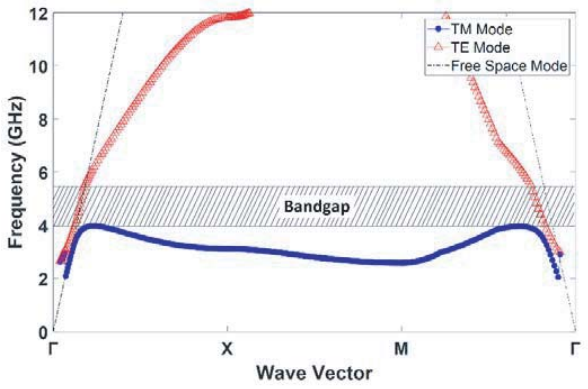

(a)

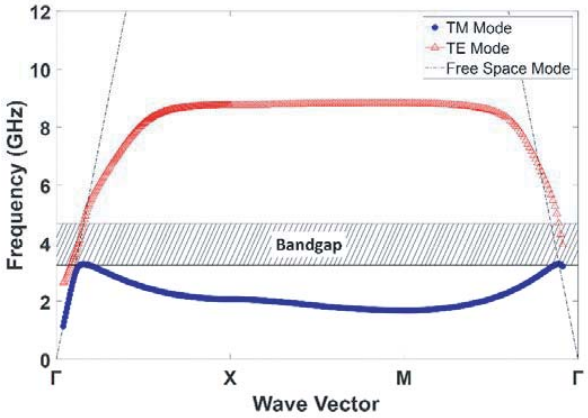

(b)

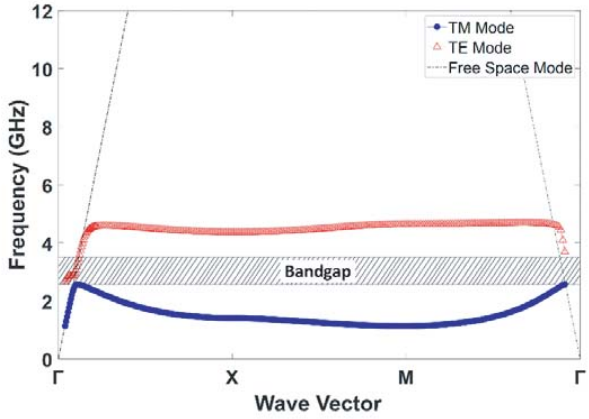

(c)

Figure 3. (a), (b), and (c) show the 2D dispersion diagram of each case for TM and TE modes. The range of their bandgaps is 3.98–5.53 GHz, 3.28–4.67 GHz, and 2.56–3.45 GHz, respectively.

After the Eigen analysis, a dispersion diagram is extracted via modal analysis to obtain the high impedance bandgap [12]. Wavevector k_x and k_y are swept along the path Γ to X band, X to M band, and M to Γ band of the irreducible Brillouin zone. Figures 3(a), (b), and (c) show the 2D dispersion diagram of each case for TM and TE modes. For all these three cases, very low group velocity is

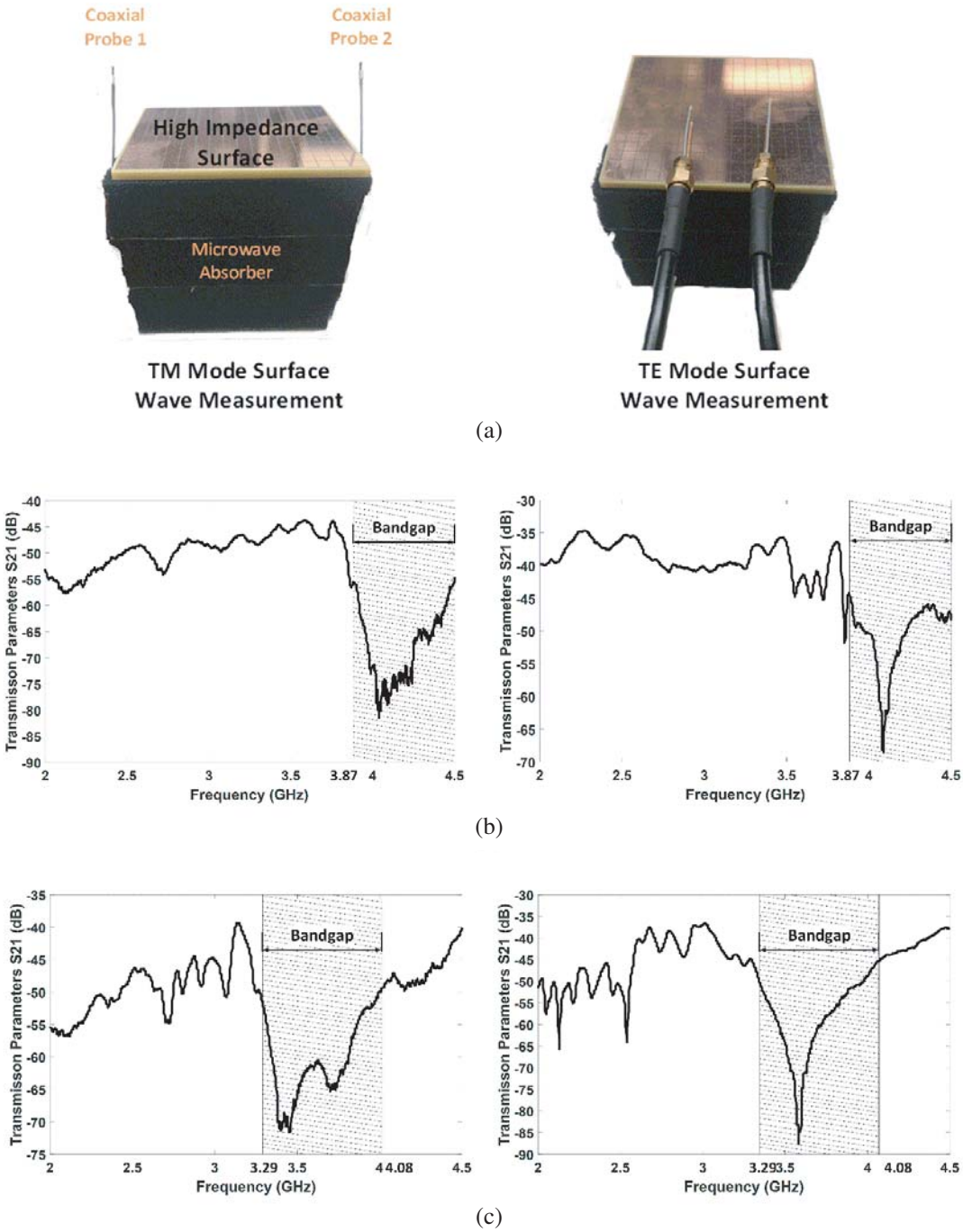

Figure 4. (a) The TM (Left) and TE (Right) surface wave measurement setup using two coaxial probe monopole antennas' S_{21} transmission coefficient. (b) Measurement data of TM (left) and TE (right) modes' S_{21} parameters, for a 16×16 three-layered mushroom-shaped high impedance surface. (c) Measurement data of TM and TE mode S_{21}, for the 16×16 surface with the proposed three-layered structure with extended current paths.

observed near the resonant frequency. For each plot, a bandgap region over which surface waves are suppressed is marked. The shift toward lower frequency ranges is due to an increase in the inductance of a unit cell associated with the extended current paths.

Numerical calculations show that the center resonance frequency for the proposed three and five-layered structure decreases by 800 MHz and 1.7 GHz, respectively. The central resonant frequency is estimated from the center of the bandgap. This suggests that a significant shift in a resonant frequency can be achieved by introducing extended current paths and the high impedance surface can be further miniaturized by the insertion of multiple inductive layers. No significant bandwidth reduction is observed from the proposed three-layer structure compared with traditional structure, while the six-layer structure's bandwidth is largely reduced due to the additional capacitive coupling result from the closely-spaced extended path.

4. EXPERIMENTAL RESULTS

We fabricate both single and three-layered mushroom-shaped high impedance surfaces using standard PCB Fabrication technology (Advanced Circuits). Each sample has 16×16 cells and their unit-cell dimension is based on Figure 1.

For the board stackup, the three-layered board consists of the top and bottom FR-4 370HR substrates (0.039 inches thickness) and the middle FR-4 substrate (0.024 inches thickness), where two B-stage (0.0075-inches thickness) applied to both sides of it to adhere FR-4 substrates together. Blind micro vias of 120 µm diameter are drilled in the top and bottom dielectric layer and buried via of the same size is drilled in the middle layer. The extended path's width on both sides of the middle layer is 240 µm.

The characteristics of each sample are measured by an Agilent vector network analyzer E5061B. The experimental setup for the surface wave measurements using coaxial probes antennas is shown in Figure 4(a). Here, two coaxial probe antennas are vertically/parallel placed to the high impedance surface (placed above the EM absorber) to capture TM and TE mode surface wave propagation and coaxial probes are connected to port 1 and port 2 of the vector network analyzer to measure the S_{21} transmission coefficient. Figures 4(b), (c) show the measured transmission coefficient of each high impedance surface. The resonant frequency of the proposed structure is 700 MHz lower than that of the reference structure as shown in Figure 4(a). These measurement data are consistent with results from numerical and analytical approaches, which verify the contribution of inductive loading to the reduction of resonant frequency and the LC modeling accuracy. Unlike the three-stacked-layer capacitive loading technique widely used to lower the resonant frequency to low gigahertz range [13], the bandwidth measured from the proposed three-layer structure is not reduced compared with the traditional design, which indicates the inductive loading technique is a better approach when the bandwidth is critical for design.

5. CONCLUSION

This report proposes a novel approach using an extended current path to lower the resonant frequency of the high impedance surface, which can be potentially used for size miniaturization in the low gigahertz frequency range. The lowering of the resonant frequency is due to an increase in the inductance of a unit cell, associated with the additional three-dimensional inductor introduced. The extended current path of the proposed mushroom-shaped high impedance surface is diagonally oriented for the isotropy characteristics. We fabricated a traditional high impedance surface and a proposed three-layered structure to demonstrate the idea, and their characteristics are verified with experiments and numerical simulations. Results revealed that a three-layered extended current path leads to a significant reduction ($\sim 20\%$ with respect to the central resonant frequency) in resonant frequency compared with traditional structures and more reduction can be achieved with a five-layered structure. The proposed platform structure can be extended to designs that incorporate many other existing inductor structures. Such demonstration provides the potential for widespread use of this technology in wireless communication or wireless power transmission.

REFERENCES

1. Sievenpiper, D., L. Zhang, R. F. Broas, N. G. Alexopolous, and E. Yablonovitch, "High-impedance electromagnetic surfaces with a forbidden frequency band," *IEEE Transactions on Microwave Theory and Techniques*, Vol. 47, No. 11, 2059–2074, 1999.
2. Clavijo, S., R. E. Diaz, and W. E. McKinzie, "Design methodology for Sievenpiper high-impedance surfaces: An artificial magnetic conductor for positive gain electrically small antennas," *IEEE Transactions on Antennas and Propagation*, Vol. 51, No. 10, 2678–2690, 2003.
3. Kim, I. K., H. Wang, S. J. Weiss, and V. V. Varadan, "Embedded wideband metaresonator antenna on a high-impedance ground plane for vehicular applications," *IEEE Transactions on Vehicular Technology*, Vol. 61, No. 4, 1665–1672, 2012.
4. Mohamed-Hicho, N. M., E. Antonino-Daviu, M. Cabedo-Fabrés, and M. Ferrando-Bataller, "A novel low-profile high-gain UHF antenna using high-impedance surfaces," *IEEE Antennas and Wireless Propagation Letters*, Vol. 14, 1014–1017, 2015.
5. Costa, F., S. Genovesi, and A. Monorchio, "A frequency selective absorbing ground plane for low-RCS microstrip antenna arrays," *Progress In Electromagnetics Research*, Vol. 126, 317–332, 2012.
6. Vallecchi, A., J. R. De Luis, F. Capolino, and F. De Flaviis, "Low profile fully planar folded dipole antenna on a high impedance surface," *IEEE Transactions on Antennas and Propagation*, Vol. 60, No. 1, 51–62, 2011.
7. Kim, S., A. Li, and D. F. Sievenpiper, "Reconfigurable impedance ground plane for broadband antenna systems," *2017 IEEE International Symposium on Antennas and Propagation & USNC/URSI National Radio Science Meeting*, 1503–1504, IEEE, July 2017.
8. Park, S. I., "Enhancement of wireless power transmission into biological tissues using a high surface impedance ground plane," *Progress In Electromagnetics Research*, Vol. 135, 123–136, 2013.
9. Bansal, A., B. C. Paul, and K. Roy, "An analytical fringe capacitance model for interconnects using conformal mapping," *IEEE Transactions on Computer-Aided Design of Integrated Circuits and Systems*, Vol. 25, No. 12, 2765–2774, 2006.
10. Grover, F. W., *Inductance Calculations: Working Formulas and Tables*, Courier Corporation, 2004.
11. Remski, R., "Analysis of photonic bandgap surfaces using Ansoft HFSS," *Microwave Journal*, Euroglobal Edition, Vol. 43, No. 9, 190–199, 2000.
12. Ashcroft, N. W. and N. D. Mermin, "Solid state physics," Saunders College, Philadelphia, 1976.
13. Costa, F., S. Genovesi, and A. Monorchio, "On the bandwidth of high-impedance frequency selective surfaces," *IEEE Antennas and Wireless Propagation Letters*, Vol. 8, 1341–1344, 2009.